

OFDM Systems Design Using Harmonic Wavelets

Kelvin Anoh[†], Augustine Ikpehai[†], Bamidele Adebisi[†], Khaled Rabie[‡], Wasiu Popoola[‡] and Haris Gacanin[§]

[†]School of Engineering, Manchester Metropolitan University, Manchester, M1 5GD, UK

[‡]Institute for Digital Communications, School of Engineering, University of Edinburgh, Edinburgh EH9 3JL, UK

[§]Nokia-Bell Labs Antwerp, Belgium

[†][k.anoh, a.ikpehai, b.adebisi, k.rabie]@mmu.ac.uk, [‡]w.popoola@ed.ac.uk, [§]haris.gacanin@nokia-bell-labs.com

Abstract—Orthogonal frequency-division multiplexing (OFDM) is a popular multi-carrier technique used in many digital communication systems such as wireless fidelity (Wi-Fi), long term evolution (LTE) and power line communication systems. It can be designed using fast Fourier transform (FFT) or wavelet transform (WT). The major drawback in using WT is that it is computationally inefficient. In this study, we introduce a simple and computationally efficient WT, harmonic wavelet transform, for OFDM signal processing. The new WT uses the orthogonal basis functions of conventional FFT-OFDM except that it involves translation and dilation of the input signal; the new wavelets is referred to as harmonic wavelets (HW). When compared with pilot-assisted OFDM system in terms of reduction in the peak-to-average power ratio, the results show that HW-OFDM outperforms FFT-OFDM by 3 dB at 10^{-4} CCDF (complementary cumulative distribution function). Over Rayleigh fading channel with additive white Gaussian noise (AWGN), the bit error ratio of both FFT-OFDM and HW-OFDM perfectly matched, showing that the proposed HW-OFDM is better in terms of peak-to-average power ratio reduction.

Index Terms—BER, Harmonic wavelet, OFDM, PAPR, pilot-assisted OFDM, Rayleigh fading, Wavelet.

I. INTRODUCTION

The study of orthogonal frequency-division multiplexing (OFDM) design using discrete Fourier transform (DFT) has been around for some time [1]. OFDM is prominent in the design of communication systems such as Wi-Fi, WiMAX, LTE and power line communication (PLC) systems. It divides wide bandwidth into many narrow bands leading to long symbol periods in time-domain and making OFDM robust against multipath fading. OFDM can be implemented using fast Fourier transform (FFT) which is the computationally efficient algorithm of DFT [2]. The FFT reduces computational complexity from $\mathcal{O}(N^2)$ to $\mathcal{O}(N \log_2 N)$ for N data symbols.

However, one of the major drawbacks of OFDM design using FFT is that it suffers from high peak-to-average power ratio (PAPR). In other words, conventional communication systems operating with FFT-OFDM leads to inefficient and costly high power amplifier (HPA). This is the major reason for not using OFDM in the uplink of mobile communication standard [3]. To solve this problem, there are different alternatives reported in the literature including single-carrier (SC) frequency-division multiple access (FDMA), fractional Fourier transform (FrFT) and wavelet transform (WT) [4]–[7]. While SC-FDMA demonstrates improved PAPR performance, FrFT and WT are computationally burdensome which may lead to

slow performing and high power consuming systems. One of the reasons why FrFT and WT may have not appeared in the wireless communication systems includes that such systems are power-limited and may cause high power consumption problems. WT is used in designing OFDM system and has better spectral leakage than filtered-OFDM as in IEEE 1901 standard commonly applied in PLC systems [8].

In this study, we present a new implementation scheme of WT that uses FFT/IFFT, initially described as harmonic wavelets (HW) [9]. HW was originally proposed to study the vibration of advanced rotating machines in mechanical vibrations and rotordynamics [10]. The main advantage of using wavelets in machine condition monitoring is that wavelet maps can produce three-dimensional (3D) plots showing amplitude, frequency and time [10]. FFT on the other hand only shows frequency (or time) and amplitude (or 2D). Wavelets show tiny changes in the frequency domain that cannot be detected in the conventional (FFT-based) frequency spectrum.

Since the HW can be implemented using the IFFT/FFT algorithm, the system model enjoys $\mathcal{O}(N \log_2 N)$ computational efficiency for the $m = \log_2(N)$ decomposition levels involved in the processing of N -long input symbol using WT. Given these advantages, we extend the new wavelet transform (i.e. HW) into the design and study of communication systems driven by OFDM and this will be referred to as HW-OFDM. In particular, this study will investigate the PAPR performance of the HW-OFDM system against that of FFT-OFDM for pilot-assisted OFDM (PA-OFDM) system. Alongside, the bit error ratio (BER) performance over Rayleigh fading channel with additive white Gaussian noise (AWGN) will be reported. Our results highlight that HW-OFDM system achieves similar BER performance with FFT-OFDM system over fading channel with AWGN. On top of that, HW-OFDM systems exhibits better reduced PAPR, up to 3 dB, than the OFDM scheme.

II. SYSTEM MODEL

Consider a signal $x[n]$, $\forall n = 0, \dots, N-1$ in time domain, its frequency domain contents $X[k]$, $\forall k = 0, \dots, N-1$ can be realized from the FFT transform of x , where n and k represent the time and frequency domains indices, respectively. The time domain OFDM signal can then be expressed as

$$x[n] = \frac{1}{\sqrt{N}} \sum_{k=0}^{N-1} X[k] \exp\left(i2\pi \frac{kn}{N}\right), \forall n, k = 0, \dots, N-1 \quad (1)$$

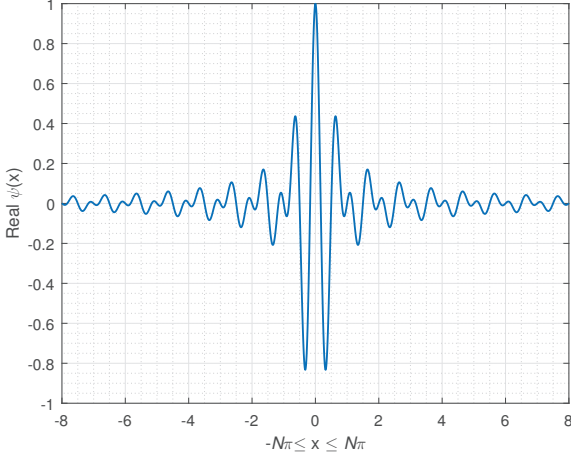


Figure 1: Real part of HW transform of a signal

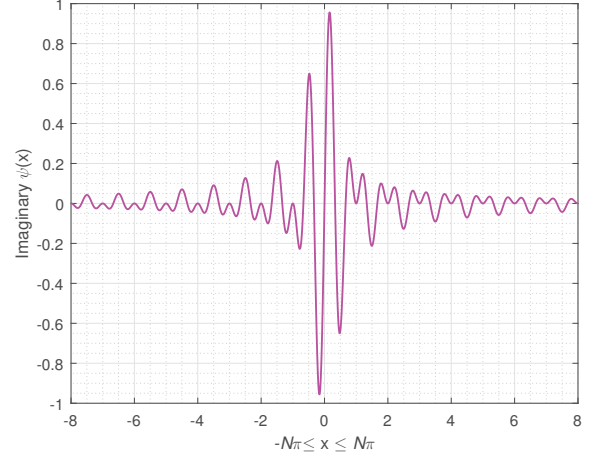


Figure 2: Imaginary part of HW transform of a signal

where $i = \sqrt{-1}$ and (1) is the conventional FFT-OFDM. Unlike DFT, WT is an alternative design kernel for implementing OFDM-like multicarrier systems. WT are made up of low-pass filters (LPF) and high-pass filters (HPF) that weight the dilated scaling function, ϕ . The LPF is related to the scaling function and both are used to realize the approximate coefficients a of the signal while the HPF is concerned with the wavelet function, ψ , both of which are used to extract the detail coefficients d of the signal.

A. OFDM Systems Design using WT

Given the time domain signal $x[n], \forall n = 0, \dots, N-1$ and $2^m \in N$, the WT of $x[n]$ are the dilated ('stretched') and translated ('repositioned') versions of $x[n]$. When only the approximate coefficient is dilated, only the discrete WT (DWT) are realized. On the other hand, when both the detail and approximate coefficients of $x[n]$ are dilated at every decomposition level, m , the wavelet packet transform (WPT) are realized. A comparative study on the performance of DWT and WPT for OFDM systems has been documented in [11]. Besides, the implementation of WPT-OFDM for multi-antenna application has also been discussed in [12].

The aim of this study is to design an OFDM system using a different kernel other than FFT/IFFT. The alternative kernel uses the DFT tool except that there exists dilation (stretching) and translation (repositioning) of the signal coefficients. Since WT finds applications in communication systems design, WT-OFDM has been studied by different authors for wireless [13]–[16] and PLC [17], [18] systems. A major drawback in its adoption is that it is computationally inefficient and recent studies have led to different computationally efficient algorithms such as the ones reported in [9] and [19]. In the following, the basics of OFDM system design using WT as an alternative kernel to FFT are discussed.

B. Wavelet and Scaling Functions of HW Transform

From Section II-A, it is observed that there are two essential parts of a WT, namely the scaling function $\phi(\cdot)$ and the

wavelet function $\psi(\cdot)$. HW transform also has these important parts and will be required in the processing of the signal. Meanwhile, the advantages of HW are that it is simple and fast to compute [10]. HW is known to be faster than other WTs and up to four times faster than Daubechies wavelets [10]. These properties make HW attractive in many applications that require low complexity and low computational cost.

The wavelet function of HW was derived in [9] as

$$\psi(x) = \frac{\exp(i4\pi x) - \exp(i2\pi x)}{i2\pi x}, \quad -\pi \leq x \leq \pi. \quad (2)$$

By observing (2) closely, one can easily separate the components of ψ into real and imaginary parts as follows

$$\psi(x) = \psi_e(x) + i\psi_o(x), \quad (3)$$

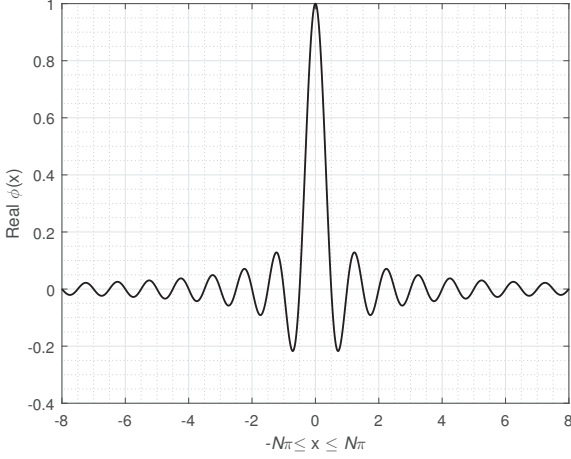
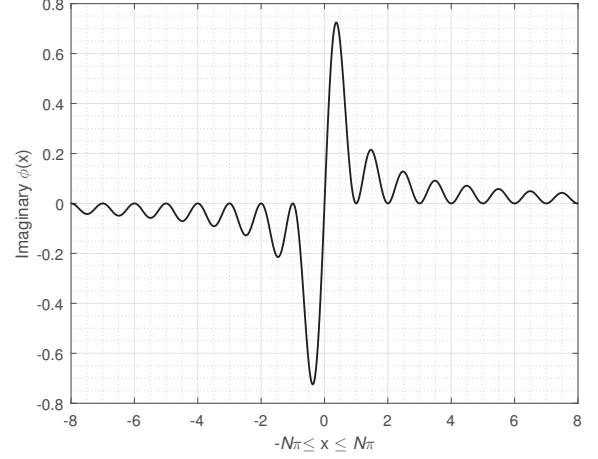
which is generally a complex number. Pictorially, $\psi_e(x)$ and $\psi_o(x)$ can be illustrated as shown in Figs. 1 and 2, respectively. It can be observed that the HW concentrates the energy of the signal (compact) around zero.

Recall that WT uses dilation and translations of signals. By replacing x in (2) with $(2^m x - t)$, the HW transform stretches x by t at each m^{th} decomposition level. The implication of $(2^m x - t)$ is that the scale of HW is compressed by the factor 2^m while its position is translated (repositioned) by t time units during every new scale. Similar to (3), the translated and dilated versions of (2) have a complex conjugate $\bar{\psi}(2^m x - t)$ given in terms of Fourier transform [20] as

$$\bar{\psi}(2^m x - t) = \frac{1}{2\pi} \int_{-4\pi 2^m}^{4\pi 2^m} \frac{1}{2^m} \exp(i\omega t/2^m) \exp(-i\omega x) d\omega \quad (4)$$

Both $\bar{\psi}(2^m x - t)$ and $\psi(2^m x - t)$ are required in the realization of the detail coefficients of x .

So far, we have only given interpretation to the d coefficients of the signal without a corresponding treatment to the a coefficients. The detail coefficients of a signal transformed (expanded) using wavelet analysis is associated with the wavelet function $\psi(\cdot)$ while the approximate part is associated with scaling function $\phi(\cdot)$. Both are required in the complete

Figure 3: Real part of $\phi(x)$ of HW transform of a signalFigure 4: Imaginary part of $\phi(x)$ of HW transform of a signal

multi-resolution analyses of a signal using wavelet theory. The scaling function can be expressed as follows [9]

$$\phi(x) = \frac{\exp(i2\pi x) - 1}{i2\pi x}, \quad -\pi \leq x \leq \pi. \quad (5)$$

Its translated version is realized from substituting x with $(x - t)$. Similar to (3), the scaling function can be decomposed into real and imaginary parts as follows

$$\phi(x) = \phi_e(x) + i\phi_o(x), \quad (6)$$

where $\phi_e(x)$ and $\phi_o(x)$, respectively are shown in Figs. 3 and 4. Similar to the case of the $\psi(\cdot)$, it can as well be noticed that the energy of the transformed signal using the $\phi(\cdot)$ is concentrated around zero (i.e. compact). In the study of HW, the scaling function $\phi(x - t)$ and its conjugate $\bar{\phi}(x - t)$ as well as the wavelet function $\psi(2^m x - t)$ and its corresponding conjugate $\bar{\psi}(2^m x - t)$ are required in the signal analyses. The decomposition and stretching lead to subchannelization. Recall that the PAPR of OFDM signal, decreases with decreasing FFT sizes. In other words, due to the subchannelization, the peak power of sub-band signals at each decomposition level will be lower than the conventional; in general, this will cause HW-OFDM to exhibit lower PAPR than FFT-OFDM.

C. Orthogonality

In designing OFDM systems, the basis functions must satisfy the condition of orthogonality. HW of different (m) decomposition levels are orthogonal; mathematically,

$$\int_{-\infty}^{\infty} \psi(x) \bar{\psi}(2^m x - t) dx = 0 \quad (7)$$

where $\bar{\psi}(\cdot)$ represents the complex conjugate of $\psi(\cdot)$. In addition, $\forall t \neq 0$, all wavelets translated by any integer t unit are orthogonal to each other. These are already proven in [9].

D. OFDM Signal from WT

In the analyses of HW, both $\phi(\cdot)$ and $\psi(\cdot)$ are usually considered; including their corresponding conjugates. This involves combining the results in (4) and (6) to process the signal, x . In that case, the output signal can be expressed as

$$f(x) = \sum_{t=-\infty}^{\infty} \{x_{(\phi,t)} \phi(x - t) + \bar{x}_{(\phi,t)} \bar{\phi}(x - t)\} + \sum_{m=0}^{\infty} \sum_{t=-\infty}^{\infty} \{x_{(\psi,t)} \psi(2^m x - t) + \bar{x}_{(\psi,t)} \bar{\psi}(2^m x - t)\}, \quad (8)$$

where $x_{(\psi,t)}$ is associated with $\psi(\cdot)$ as follows [20]

$$\begin{aligned} x_{(\psi,t)} &= 2^m \int_{-\infty}^{\infty} f(x) \bar{\psi}(2^m x - t) dx \\ &= \sum_{v=0}^{2^m-1} X_{(2^m+v)} \exp\left(\frac{i2\pi vt}{2^m}\right) \quad \forall t = 0, 1, \dots, 2^m - 1. \end{aligned} \quad (9)$$

Clearly, (9) is the inverse Fourier transform of $X_{(2^m+v)}$ which can be implemented using IFFT. Similarly, the amplitude of the corresponding complex conjugate of the wavelet can be written as

$$\begin{aligned} \bar{x}_{(\psi,t)} &= 2^m \int_{-\infty}^{\infty} f(x) \psi(2^m x - t) dx \\ &= \sum_{v=0}^{2^m-1} X_{-(2^m+v)} \exp\left(-\frac{i2\pi vt}{2^m}\right). \end{aligned} \quad (10)$$

By using the circular property of DFT, it can be remarked that

$$X_{(-v)} = X_{(N-v)}, \quad \forall v = 0, 1, \dots, 2^m - 1. \quad (11)$$

Based on (11), we can rewrite (10) as follows

$$\begin{aligned} \bar{x}_{(\psi,t)} &= \sum_{v=0}^{2^m-1} X_{N-(2^m+v)} \exp\left(-\frac{i2\pi vt}{2^m}\right) \\ &\quad \forall t = 0, 1, \dots, 2^m - 1. \end{aligned} \quad (12)$$

We also see that (12) can be implemented using FFT.

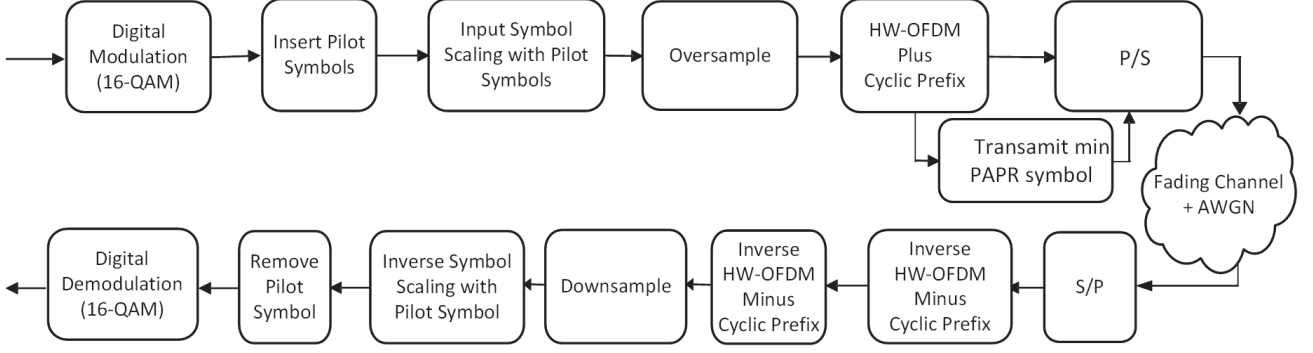


Figure 5: Block diagram for implementing HW-OFDM (P/S: parallel to serial conversion and S/P: serial to parallel conversion).

The approximate coefficients, namely $x_{(\phi,t)}$ and $\bar{x}_{(\phi,t)}$ are obtained from $\bar{\phi}(\cdot)$ and its complex conjugate $\phi(\cdot)$, respectively. From the foregoing discussion,

$$\begin{aligned} x_{(\phi,t)} &= 2^m \int_{-\infty}^{\infty} f(x) \bar{\phi}(x-t) dx \\ &= \int_0^{2\pi} X(\omega) \exp(i\omega t) d\omega, \end{aligned} \quad (13)$$

where $X(\omega) = \int_{-\infty}^{\infty} f(x) e^{-i\omega x} d\omega$ and the scaling function is

$$\phi(x-k) = \int_{-\infty}^{\infty} \Phi(\omega) e^{-i\omega k} e^{i\omega x} d\omega. \quad (14)$$

Note that $\Phi(\omega) = 0$ except for $0 \leq \omega < 2\pi$. By letting $X(\omega = 0)$ be replaced with X_0 , $x_{(\phi,t)} = X_0/2$ and $\bar{x}_{(\phi,t)} = X_0/2$ so that

$$x_0 = x_{(\phi,t)} + \bar{x}_{(\phi,t)} = X_0. \quad (15)$$

Lastly, to ensure that Parseval's theorem holds i.e., $\frac{1}{2^m} \sum_{t=0}^{2^m-1} |x_{2^m+t}|^2 = \sum_{t=0}^{2^m-1} |X_{2^m+t}|^2$, we set

$$x_{N/2} = X_{N/2}. \quad (16)$$

In summary, we require only (9), (12), (15) and (16) to implement the HW transform in OFDM design. Useful MATLAB codes that implement HW transform can be found in [20].

E. Pilot-Assisted OFDM from HW-OFDM Symbol

PAPR reduction in OFDM systems is an important tool for increasing the power efficiency of HPA in digital communication systems. OFDM symbols exhibit high peaks which may appear within the nonlinear region of operation of HPAs. By reducing these peaks to reside within the linear region, HPA consume less power. There are different techniques in the literature for reducing the PAPR performance of OFDM systems. Examples include clipping [21], [22], companding [23], [24] and use of pilot symbols [18], [25]. In this study, pilot symbols scheme applied to reduce the PAPR in wavelet-OFDM system in [18] is adopted. By using pilot symbols, no additional overhead is introduced to the system since the pilot-symbols are used also for channel estimation purposes [25]. The system model is shown in Fig. 5. Consider some frequency domain

symbols, $D_{\bar{n}}$ and some pilot symbols $M_{\tau}^u = A_{\tau,u} \exp(i\theta_{\tau,u})$, we express the modified symbol as

$$\bar{X}_{\bar{n}} = D_{\bar{n}} \otimes M_{\tau}^u \quad \forall \tau \in P, \bar{n} \in N - P, \quad (17)$$

where A_{τ}^u , $\forall u = 1, \dots, U$ is the amplitude of M_{τ}^u with phase $\theta_{\tau,u}$, $\forall \bar{n} = 0, 1, \dots, N - P$ and $\bar{X}_{\bar{n}} \in \mathbb{C}^{(N-P) \times 1}$. In (17), the amplitudes of the pilot symbol, $A_{\tau,u}$, scale the amplitudes of frequency domain content of the HW-OFDM signal while the phase of the frequency domain content of the HW-OFDM is rotated by $\theta_{\tau,u}$ which are drawn from $\theta_{\tau,u} = [0, \pi]$. After that, the pilot symbols which can be used for channel estimation are inserted as follows [26]

$$X_j = \bar{X}_{\bar{n}} + \bar{X}_{p,j}^u, \quad \forall j = 0, 1, \dots, N - 1, \quad (18)$$

where P is the number of pilots and $u \in U$ is the pilot sequence. After these, the HW-OFDM pilot-aided symbol is oversampled by a factor ℓ to ensure that none of the symbol peaks is missed out, such that

$$X_n = [X_j \quad \mathbf{0}_{1 \times \ell N - N}] \quad \forall n = 0, 1, \dots, \ell N - 1. \quad (19)$$

The HW-OFDM that will be transmitted over the channel which includes pilot symbols and oversampling can be expressed as

$$s[n] = \mathbf{W}(X_n) \quad \forall n = 0, 1, \dots, \ell N - 1, \quad (20)$$

where $\mathbf{W}(\cdot)$ is the HW transform of the input symbol which is expressed in (8). Next, the signal that achieves the minimum PAPR among $r = 1, 2, \dots, \bar{r}$ iterations from the following

$$\bar{s}_{p,r}^u[n] = \min_{1 \leq r \leq \bar{r}} (\text{PAPR}_{p,r}^u) \quad \forall u = 1, \dots, U \quad (21)$$

will be transmitted over the fading channel. In (21), the PAPR of the pilot-assisted HW-OFDM signal can be determined as

$$\text{PAPR}_{p,r}^u = \frac{\max_{n=0, \dots, \ell N - 1} \{|\bar{s}_{p,r}^u[n]|^2\}}{\mathbb{E}\{|\bar{s}_{p,r}^u[n]|^2\}}, \quad (22)$$

where $\mathbb{E}\{\cdot\}$ is the expected value operator. Usually, the PAPR is reported in terms of CCDF and can be expressed as

$$\Pr\{\text{PAPR} > \text{PAPR}_0\} = [1 - \{1 - \exp(-\text{PAPR})\}^{\ell N}], \quad (23)$$

where $\Pr\{\cdot\}$ represents the probability of $\{\cdot\}$.

The OFDM symbol that exhibits the minimum PAPR is then obtained and transmitted over the fading channel. Supposing

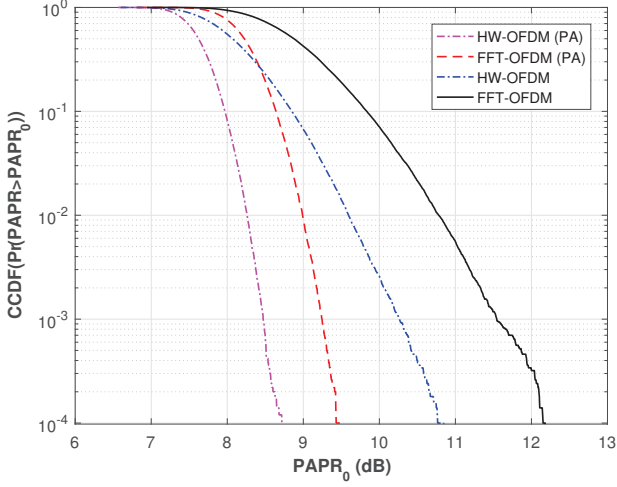


Figure 6: PAPR performance of pilot-assisted HW-OFDM in comparison with FFT-OFDM ($\ell = 4$, 16QAM and $N = 128$)

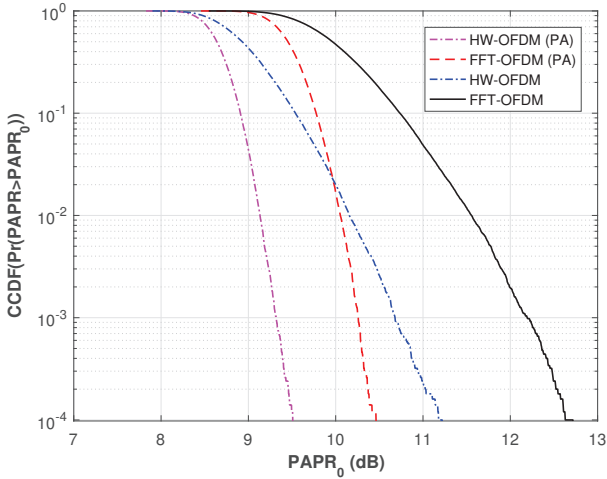


Figure 7: PAPR performance of pilot-assisted HW-OFDM in comparison with FFT-OFDM ($\ell = 4$, 16QAM and $N = 1024$)

that the fading channel follows the Rayleigh distributions with variance σ_h^2 . The received signal in frequency domain after the cyclic prefix is removed can be expressed as: $Y = HX + Z$ where H is the channel transfer function and X is the transmitted signal. The recovered signal after equalization can be written as

$$\bar{X} = \mathcal{H}_{MMSE} \cdot Y = X + \frac{H^*}{|H^*|^2 + \left(\frac{E_x}{N_0}\right)^{-1}} Z, \quad (24)$$

where $Z \sim \mathcal{N}(0, \sigma_z^2)$ is the AWGN and \mathcal{H}_{MMSE} is the minimum mean square error (MMSE) channel equalizer given by $H^* / \left(|H^*|^2 + \left(\frac{E_x}{N_0}\right)^{-1} \right)$. (24) is the MMSE estimate of the transmitted OFDM symbol. MMSE equalization is used because it has the potential to minimize the impact of noise on the received signal.

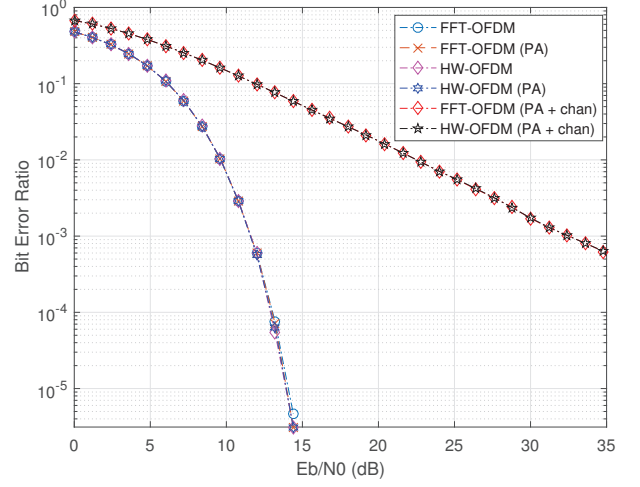


Figure 8: BER performance of HW-OFDM in comparison with FFT-OFDM over a Rayleigh fading channel with AWGN ($\ell = 4$, $M = 16$ QAM and $N=128$)

III. SIMULATION RESULTS AND DISCUSSION

To demonstrate the performance of the proposed HW-OFDM relative to FFT-OFDM, we conducted an investigation using the model shown in Fig. 5. The model used in the simulation involves $N = 128$ randomly generated input symbol which are digitally modulated using 16-QAM (quadrature amplitude modulation). Signals realized from this process were scaled to ensure that $\mathbb{E}\{|s[n]|\} \approx 1$. Afterwards, pilot symbols with property as discussed in Section II-E are constructed and inserted within the HW-OFDM symbol before transmission over the channel. The PAPR of the output symbols is estimated using (22). As shown in Fig. 5, only the HW-OFDM symbol with the minimum PAPR value among $r = 1, \dots, \bar{r}$ are transmitted over the channel. The fading channel assumes the Rayleigh distribution in which the channel state information are known at the receiver. At the receiver, we adopted MMSE equalization technique to recover the transmitted signals as shown in (24). These processes are repeated for $N = 1024$ and the results obtained over the Rayleigh fading channel with AWGN are reported in terms of BER in Figs. 8 and 9.

We find in Fig. 6 that the PAPR performance of HW-OFDM is lower than that of standard FFT-OFDM system by about 0.5 dB. When the phase and amplitudes ($A_i^u = 1$) of the pilot symbols are exploited, this PAPR reduction further improves by an additional 2.5 dB at 10^{-4} CCDF. Fundamentally, increasing the number of OFDM sub-carriers increases PAPR degradation as also seen when comparing Figs. 6 and 7. However, by increasing the number of sub-carriers from $N = 128$ to $N = 1024$ for the two schemes, it is seen that the proposed HW-OFDM further reduces the PAPR by 3 dB at 10^{-4} CCDF relative to FFT-OFDM. Due to varying number of subchannels (which are smaller than N) at each decomposition level, the DFT of the Gaussian variable in the HW transform enables lower peak power than conventional DFT, and thus HW-OFDM exhibits lower PAPR than FFT-OFDM.

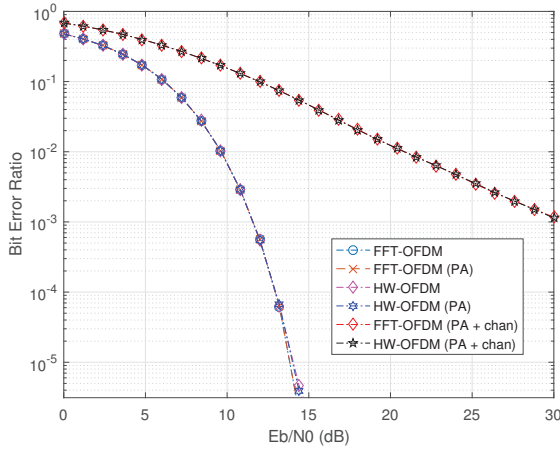


Figure 9: BER performance of HW-OFDM in comparison with FFT-OFDM over a Rayleigh fading channel with AWGN ($\ell = 4$, $M = 16$ QAM and $N=1024$)

In terms of BER performance, the FFT-OFDM and the HW-OFDM are seen to perform similarly at all E_b/N_0 shown. Typically, PAPR reduction that uses symbol phase rotation has negligible impacts on the BER performance. We can see that although the proposed pilot-assisted scheme reduces the PAPR, it does not degrade the BER performances of the FFT-OFDM and HW-OFDM systems. However, as shown in Figs. 8 and 9, the results show that the BER performance is degraded when compared to the AWGN-only channel; this is expected due to the impacts of the dispersive channel on the OFDM symbols and the noise that is magnified due to channel estimation. One of the ways of improving this performance is through forward error correction.

IV. CONCLUSION

In this study, we have demonstrated a new WT design scheme for processing OFDM symbols. The HW was implemented using the FFT/IFFT algorithm (that requires $\mathcal{O}(N \log_2 N)$ hence computationally efficient) and uses only $m = \log_2(N)$ decomposition levels given a data symbol of length N . The design kernel is the HW and was found to exhibit 3dB better in PAPR performance than FFT-based OFDM. Over Rayleigh fading channels, we observed that the model performs similarly as the FFT-based OFDM in terms of BER. Since the HW-OFDM has equivalent BER performance as the FFT-OFDM and uses the FFT/IFFT tool, the HW-OFDM scheme can be applied in the design of communication systems henceforth; both wireless and wired. In the future, we shall assess the performance of the proposed kernel with other alternative design kernels for OFDM systems.

REFERENCES

[1] S. Weinstein and P. Ebert, "Data Transmission by Frequency-Division Multiplexing Using the Discrete Fourier Transform," *IEEE Trans. Commun. Technol.*, vol. 19, no. 5, pp. 628–634, Oct. 1971.

[2] R. N. Bracewell, *The Fourier transform and its applications*. McGraw-Hill New York, 1986, vol. 31999.

[3] G. Wunder, R. F. H. Fischer, H. Boche, S. Litsyn, and J.-S. No, "The PAPR problem in OFDM transmission: New directions for a long-lasting problem," *IEEE Signal Process. Mag.*, vol. 30, no. 6, pp. 130–144, 2013.

[4] D. Mendlovic, Z. Zalevsky, and D. e. a. Mas, "Fractional wavelet transform," *Applied optics*, vol. 36, no. 20, pp. 4801–4806, 1997.

[5] J. Shi, N. Zhang, and X. Liu, "A novel fractional wavelet transform and its applications," *Science China Info. Sciences*, vol. 55, no. 6, pp. 1270–1279, 2012.

[6] M. Martone, "A multicarrier system based on the fractional fourier transform for time-frequency-selective channels," *IEEE Trans. Commun.*, vol. 49, no. 6, pp. 1011–1020, Jun. 2001.

[7] K. O. O. Anoh, R. A. A. Alhameed, and S. M. R. Jones, "An investigation of FrFT modulation and FFT-OFDM for multiple input multiple output application," in *14th Annual Post Graduate Symposium on Convergence of Telecom., Network. Broadcast.*, 2013.

[8] A. Farhang, M. M. Kakhki, and B. Farhang-Boroujeny, "Wavelet-OFDM versus filtered-OFDM in power line communication systems," in *2010 5th Intl. Symposium Telecom.*, Dec. 2010, pp. 691–694.

[9] D. E. Newland, "Harmonic wavelet analysis," *Proc. R. Soc. Lond. A*, vol. 443, no. 1917, pp. 203–225, 1993.

[10] J. I. Bonel-Cerdan and J. L. Nikolajsen, "An introduction to harmonic wavelet analysis of machine vibrations," in *ASME 1997 Intl. Gas Turbine and Aeroengine Congress and Exhibition*. American Society of Mechanical Engineers, 1997, pp. V004T14A011–V004T14A011.

[11] O. O. Anoh, N. T. Ali, R. Abd-Alhameed, S. M. R. Jones, and Y. A. S. Dama, "On the performance of DWT and WPT modulation for multicarrier systems," in *2012 IEEE 17th Intl. Workshop on Computer Aided Modeling and Design of Commun. Links and Networks (CAMAD)*, Sept. 2012, pp. 348–352.

[12] K. O. O. Anoh, R. A. Abd-Alhameed, J. M. Noras, and S. M. R. Jones, "Wavelet packet transform modulation for multiple input multiple output applications," *Intl. J. Computer Appl.*, vol. 63, no. 7, pp. 46–51, 2013.

[13] M. K. Lakshmanan and H. Nikookar, "A review of wavelets for digital wireless commun," *WPC*, vol. 37, no. 3-4, pp. 387–420, 2006.

[14] K. O. O. Anoh, J. M. Noras, R. A. Abd-Alhameed, S. M. R. Jones, and K. N. Voudouris, "A new approach for designing orthogonal wavelets for multicarrier applications," *AEU-Intl. J. Electron. Commun.*, vol. 68, no. 7, pp. 616–622, 2014.

[15] K. O. O. Anoh, T. T. Mapoka, R. A. Abd-Alhameed, O. Ochonogor, and S. M. R. Jones, "On the application of raised-cosine wavelets for multicarrier systems design," *Intl. J. Commun. and Propagation (IRECAP)*, vol. 4, no. 4, pp. 143–150, Aug. 2014.

[16] K. O. O. Anoh, R. A. Abd-Alhameed, O. Ochonogor, Y. A. S. Dama, S. M. R. Jones, and T. T. Mapoka, "Performance evaluation of raised-cosine wavelet for multicarrier applications," *Intl. J. Environmental Engineering*, vol. 1, no. 3, pp. 1–5, Sept. 2014.

[17] S. Galli, H. Koga, and N. Kodama, "Advanced signal processing for ples: Wavelet-OFDM," in *IEEE ISPLC 2008*, 2008, pp. 187–192.

[18] K. Anoh, A. Ikpehai, K. Rabie, B. Adebisi, and W. Popoola, "PAPR reduction of wavelet-OFDM systems using pilot symbols," in *2018 IEEE ISPLC*, Apr. 2018, pp. 1–6.

[19] S. G. Mallat, "A theory for multiresolution signal decomposition: the wavelet representation," *IEEE Trans. Pattern Analysis and Machine Intelligence*, vol. 11, no. 7, pp. 674–693, 1989.

[20] D. E. Newland, *An introduction to random vibrations, spectral & wavelet analysis*. Courier Corporation, 2012.

[21] X. Li and L. J. Cimini, "Effects of clipping and filtering on the performance of OFDM," in *1997 IEEE 47th Veh. Technol. Conf. Technol. in Motion*, vol. 3, May 1997, pp. 1634–1638 vol.3.

[22] K. Anoh, C. Tanriover, B. Adebisi, and M. Hammoudeh, "A new approach to iterative clipping and filtering PAPR reduction scheme for OFDM systems," *IEEE Access*, vol. 6, pp. 17 533–17 544, Sept. 2018.

[23] B. Adebisi, K. Anoh, and K. M. Rabie, "Enhanced nonlinear companding scheme for reducing PAPR of OFDM systems," *IEEE Systems J.*, vol. PP, no. 99, pp. 1–11, Jul. 2018.

[24] B. Adebisi, K. Anoh, K. M. Rabie, A. Ikpehai, M. Fernando, and A. Wells, "A new approach to peak threshold estimation for impulsive noise reduction over power line fading channels," *IEEE Systems J.*, vol. PP, no. 99, pp. 1–12, Mar. 2018.

[25] W. O. Popoola, Z. Ghassemloooy, and B. G. Stewart, "Pilot-assisted PAPR reduction technique for optical OFDM communication systems," *J. Lightwave Technol.*, vol. 32, no. 7, pp. 1374–1382, Apr. 2014.

[26] K. Wesolowski, "On the PAPR minimization using selected mapping algorithm in pilot-assisted OFDM systems," in *European Wireless Conference*, 2007.